UNESCO Chair on
Coastal Geo-Hazard Analysis
Research Institute for Earth Sciences
Geological Survey of Iran
unesco
Chair

Abstract:

Geometric and seismic parameters of the Qoshadagh Fault (QDF) were investigated to evaluate seismic hazard along this fault, which consists of three segments. The central E–W striking, dextral-reverse segment is the longest and terminates at both ends into NW–SE striking splay arrays. Both eastern and western splay arrays form locally transtensional bends. Paleoseismic data obtained from three excavated trenches across the fault combined with dated offset geomorphic features revealed that the central segment experienced at least 5 surface rupturing earthquakes during the past 2.5 ka, with maximum moment magnitude of Mw = 6.8 ± 0.2. The mean recurrence interval for the identified paleoearthquakes is 452 ± 143 years (±2σ) and the calculated amount of slip per event is ca. ≈ 0.85 m. These results imply that the QDF slips at an average rate of 1.9 ± 0.1 mm yr–1 for over the past 2.5 ka. The obtained values define the seismic behavior of the fault and are essential to remediate ensuing seismic risks.

ISBN: 978-622-5858-50-3
9 786225 858503

2023

unesco
Chair
UNESCO Chair on
Coastal Geo-Hazard Analysis
Research Institute for Earth Sciences
Geological Survey of Iran

UNESCO Chair on
Coastal Geo-Hazard Analysis
Research Institute for Earth Sciences
Geological Survey of Iran
unesco
Chair

Structual Characteristics, Paleoseismology and Slip Rate of the Qoshadagh Fault, Northwest of Iran

UCCGHA 012

2023

Structural Characteristics, Paleoseismology and Slip Rate of the Qoshadagh Fault, Northwest of Iran

سرشناسه : فریدی، محمد، ۱۳۴۵-
-Faridi, Mohammad, 1966

عنوان و نام پدیدآور : Structural characteristics, paleoseismology and slip rate of the Qoshadagh fault, Northwest of Iran[Book]/ Authors Mohammad Faridi...[et al.]; employer Research Institute for Earth Sciences; advisor Geological Survey of Iran; supervisors Hamid Nazari...[et al.]; with cooperation UNESCO Chair on Coastal Geo-Hazard Analysis; summarized Manouchehr Ghorashi.

مشخصات نشر : تهران: نشرخزه، ۱۴۰۲= ۲۰۲۳م.

مشخصات ظاهری : ۷۴ ص.: مصور(بخشی رنگی)، جدول، نمودار؛ ۱۴ × ۲۱ س‌م.

شابک : 978-622-5858-50-3

وضعیت فهرست نویسی : فیپا

یادداشت : زبان: انگلیسی.

یادداشت : عنوان به فارسی: ویژگی های ساختاری، پارینه زلزله شناسی و نرخ لغزش گسل گوشه داغ، شمال غرب ایران.

یادداشت : Authors Mohammad Faridi, Negar Haghipour, Mohammad Ali Shokri, Elaheh Ahmadzadeh, S.S. Sahebari.

یادداشت : Supervisors Hamid Nazari, Jean-Pierre Burg, Morteza Talebian, Manouchehr Ghorashi

موضوع : دیرینه لرزه شناسی

موضوع : Paleoseismology

موضوع : زمین‌شناسی -- ایران

موضوع : Geology -- Iran

موضوع : گسله‌ها -- ایران

موضوع : Faults (Geology) -- Iran

شناسه افزوده : حقی پور، نگار، شکری، محمد علی، احمدزاده، الهه، صاحباری، س.

شناسه افزوده : Negar Haghipour, Mohammad Ali Shokri, Elaheh Ahmadzadeh, S.S. Sahebari

شناسه افزوده : یونسکو. کرسی مخاطرات زمین شناختی ساحلی

شناسه افزوده : UNESCO Chair on Coastal Geo-Hazard Analysis

شناسه افزوده : سازمان زمین‌شناسی و اکتشافات معدنی کشور. پژوهشکده علوم زمین

شناسه افزوده : Geological Survey of Iran, Research Institute for Earth sciences

رده بندی کنگره : ۲/QE۵۳۹

رده بندی دیویی : ۲۲/۵۵۱

شماره کتابشناسی ملی : ۹۳۶۷۸۸۹

Structural Characteristics, Paleoseismology and Slip Rate of the Qoshadagh Fault, Northwest of Iran

Author: Mohammad Faridi

نشرخزه

اطلاعات گزارش

عنوان: ویژگی های ساختاری، پارینه زلزله شناسی و نرخ لغزش گسل گوشه داغ، شمال غرب ایران

مجری: پژوهشکده علوم زمین

مشاور: سازمان زمین شناسی و اکتشافات معدنی کشور

زبان مرجع: انگلیسی

خروجی: گزارش، نقشه، مقاله، داده های الکترونیکی

ناظران علمی: حمید نظری، ژان پیر بورگ، مرتضی طالبیان، منوچهر قرشی

نویسندگان: محمد فریدی، نگار حقی پور، محمدعلی شکری، الهه احمدزاده، صاحباری

رئیس کرسی یونسکو در مخاطرات زمین شناختی ساحلی: حمید نظری

مسئول شورای اجرایی: راضیه لک

خلاصه‌نویسی: منوچهر قرشی

ناشر: نشر خزه

با همکاری کرسی یونسکو در مخاطرات زمین شناختی ساحلی

چاپ اول: ۱۴۰۲

شمارگان: ۵۰ نسخه

صفحات: ۷۴

شابک: ۹۷۸-۶۲۲-۵۸۵۸-۵۰-۳

khazepub@gmail.com

Report Information

Title: Structural Characteristics, Paleoseismology and Slip Rate of the Qoshadagh Fault, Northwest of Iran

Employer: Research Institute for Earth Sciences

Advisor: Geological Survey of Iran

Original language: English

Output: Report, Map, Papers, Digital meta data

Supervisors: Hamid Nazari, Jean-Pierre Burg, Morteza Talebian, Manouchehr Ghorashi

Authors: Mohammad Faridi, Negar Haghipour, Mohammad Ali Shokri, Elaheh Ahmadzadeh, S.S. Sahebari

Chairholder in the UNESCO Chair on Coastal Geo-Hazard Analysis: Hamid Nazari

Head of the Executive Council: Razyeh Lak

Summarized: Manouchehr Ghorashi

Publisher: Khazeh Publication

with cooperation UNESCO Chair on Coastal Geo-Hazard Analysis

First Edition: 2023

Edition number: 50

Page: 74

Shabak: 978-622-5858-50-3

khazepub@gmail.com

Scientific Council

Name	Affiliation
Ara Avagyan	IGS: Institute Geological Sciences
Rick J Bailey	IOC-UNESCO Indian Ocean Tsunami Warning and Mitigation System/ UNESCO
Aram Fathian Baneh	University of Calgary
Wenjiao Xiao	Chinese Academy of Sciences
Philippe Agard	University of Sorbonne
Eric Barrier	University of Sorbonne
Justin Ahanhanzo	Intergovernmental Oceanographic Commission of UNESCO (IOC-UNESCO)
Alice Aurelie	UNESCO Water Sciences Division
Klaus Reicherter	Aachen University
Judith Thomalsky	German Archaeological Institute Tehran Branch
Martin Hanz	German under water archaeology association
Hamid Alizadeh Lahijani	Iranian National Institute for Oceanography and Atmospheric Science
Yahya Djamour	Shahid Beheshti University (SBU)
Hassan Fazeli Nashli	University of Tehran
Razyeh Lak	Research Institute for Earth Sciences
Mohammad Mokhtari	International Institute of Earthquake Engineering and Seismology
Hamid Nazari	Research Institute for Earth Sciences

Jafar Omrani	Geological Survey of Iran
Mohammad Tatar	International Institute of Earthquake Engineering and Seismology
Morteza Talebian	Research Institute for Earth Sciences
Mehdi Zare	International Institute of Earthquake Engineering and Seismology
Stefano Salvi	National Institute of Geophysics and Volcanology (INGV)
Ryo Anma	Tokushima University
John Lambert	Deltares, UNESCO
Issa El-Hussain	Sultan Qaboos University
Egor Krasinskiy	Underwater research center Russian Geographical Society
Richard Walker	University of Oxford
Audemard Franck A.	Department of Geology, Central University of Venezuela
Wenjiao Xiao	Chinese Academy of Sciences
Jean-François Ritz	University of Montpellier
Ekkehard Holzbecher	German University of Technology in Oman
Yeong Bae Seong	Korea University

Executive Committee

Name	**Affiliation**
Dr. Razyeh Lak	Head of RIES and Executive Manager
Mahmoudreza Majidifard	Research Institute for Earth Sciences
Manouchehr Ghorashi	Research Institute for Earth Sciences
Alireza Vaezi	Research Institute for Earth Sciences
Arash Amini	Golestan University

Mohammad Tatar	International Institute of Earthquake Engineering and Seismology
Mohammad reza Ghasemi	Research Institute for Earth Sciences
Jafar Hassanpour	University of Tehran
Ataollah Dadashpour	Geological Survey of Iran, Sari branch
Ahmadreza Rabani	University of Science and Technology of Mazandaran
Ahmad Rashidi	International Institute of Earthquake Engineering and Seismology
Masoud Sadri Nasab	University of Tehran
Hasan Fazelinashli	University of Tehran
Abdolazaim Ghanghormeh	Golestan University
Ataollah Kavian	Environmental Protection Organization of Mazandaran Province
Seyed Mohsen Mortazavi	Hormozgan University
Nasir Ahmadi	Environmental Protection Organization of Mazandaran Province
Hasan Nasrollah Zadeh Saravi	Caspian Sea Ecological Research Center
Mojtaba Yamani	University of Tehran
Ahmed Hadidi	German University of Technology in Oman (GUTECH)
Alireza Amrikazemi	Scientific Coordinator, Qeshm Island UNESCO Global Geopark
Mahdi Rahmanian	Shargh Daily newspaper
Mohammad Salamati	Respina Company
Mohammadreza Kazemzadeh	Superme Audit Gourt

Secretariat

Name	Affiliation
Elnaz Aghaali	Research Institute for Earth Sciences
Hamoon Memarian	Research Institute for Earth Sciences
Hourieh AliBeygi	Research Institute for Earth Sciences
Shirin Zarei	Research Institute for Earth Sciences
Keivan Ajdari	Research Institute for Earth Sciences
Sedigheh Ghanipour	Research Institute for Earth Sciences
Shirin Safavi	Research Institute for Earth Sciences
Leila Shirazi	Research Institute for Earth Sciences
Aazam Takhtchin	Research Institute for Earth Sciences
Hanieh Bakhshaei	Geological Survey of Iran
Reza Behbahani	Geological Survey of Iran
Javad Darvishi khatooni	Geological Survey of Iran
Mohammadreza Ensani	Geological Survey of Iran
Marziyeh Estrabi Ashtiyani	Geological Survey of Iran
Gholamreza Hoseinyar	Geological Survey of Iran
Mojtaba Kavianpour Sangno	Geological Survey of Iran
Mehrnoosh Pour Saeid	Graphic Designer

Contents

Table of Figures

Abstract

Geometric and seismic parameters of the Qoshadagh Fault (QDF) were investigated to evaluate seismic hazard along this fault, which consists of three segments. The central E–W striking, dextral-reverse segment is the longest and terminates at both ends into NW–SE striking splay arrays. Both eastern and western splay arrays form locally transtensional bends. Paleoseismic data obtained from three excavated trenches across the fault combined with dated offset geomorphic features revealed that the central segment experienced at least 5 surface rupturing earthquakes during the past 2.5 ka, with maximum moment magnitude of Mw = 6.8 ± 0.2. The mean recurrence interval for the identified paleoearthquakes is 452 ± 143 years (±2σ) and the calculated amount of slip per event is ca. ≈0.85 m. These results imply that the QDF slips at an average rate of 1.9 ± 0.1 mm yr–1 for over the past 2.5 ka. The obtained values define the seismic behavior of the fault and are essential to remediate ensuing seismic risks.

INTRODUCTION

Strike slip faulting is a prominent tectonic regime in mature collisional belts (Trifonov, 1995 ; Trifonov & Kozhurin, 2010). The formation and reactivation of strike slip faults and consequent movement of large continental masses in northwest Iran is mainly attributed to ongoing, bulk N-S shortening in response to convergence between the Arabian and Eurasian plates (Rizza et al., 2013 ; Vernant, 2015). Since the region is densely populated, seismic hazard and risk evaluations are critical social needs. The dramatic earthquake of November 13, 2017 in Kermanshah City (west of Iran) is a cruel reminder. Precise mapping, geometry, determination of slip directions and estimation of seismic parameters are important steps toward the understanding of active faulting and subsequent mitigation of seismic risks. A major goal is to provide new data on structural and paleoseismolgical characteristics of the Qoshadagh Fault (QDF) as an active but unnoticed seismic source. The 11 August, 2012 destructive Varzegan – Ahar earthquake duplet occurred in NW Iran on a previously overlooked seismic source. Therefore, the event prompted new research for a comprehensive consideration of the fault in terms of structural geology, kinematic and dynamic (Copley et al., 2013 ; Ghods et al., 2015). The first field investigations and kinematic analysis divided the QDF into three segments: the E–W striking, central (main) segment and the NW–SE striking western and eastern segments. The August 11, 2012 earthquake produced ca. 15 km long surface rupture along the central segment (Copley et al., 2013 ; Faridi et al., 2017). Three trenches were excavated across the surface rupture to constrain the long-term activity of this fault segment. The stratigraphy, unconformities, sedimentary and deformational structures exposed on trench walls were logged directly by gridding and mapping in 1 : 20 scale. Trench walls were sampled and analyzed at the ETH-Zurich “^{14}C” and UNIL (University Lausanne) “OSL” laboratories to date as precisely as possible the identified ruptures and to estimate an average slip rate of the fault. Morphotectonic features were measured and combined with trench data to define fault slip parameters.

TECTONIC SETTING

The QDF is one of the active structural elements of the Azarbaijan region in Northwest Iran (Fig. 1). The region is a segment of the Alpine-Himalayan collisional belt (Alavi, 2007 ; Dewey et al., 1973 ; Ricou, 1994 ; Sengor et al., 1988). Closure of the Tethys Ocean and subsequent initiation of continental collision is Late Eocene–Oligocene (Agard et al., 2011). Roughly northward motion of the Arabian plate resulted in oblique convergence between Arabia and Iran (*Figure 1a*) so that Northwest Iran undergoes regional transpression (Mesbahi et al., 2016). The rate of convergence between Arabian and Iranian parts of Eurasia decreased considerably during the last couple of million years which is related to tectonic re-organization due to different causes, such as break-off of the Neo-Tethyan oceanic slab or the closure of the free face at the eastern margin of the collision zone (Allen et al., 2004 ; Allen et al., 2013 ; McClusky et al., 2002).

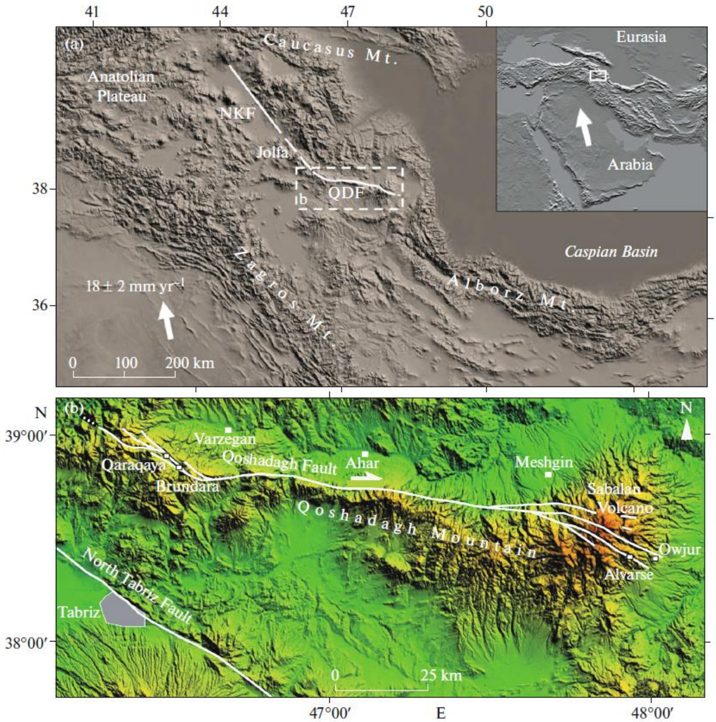

Figure 1: (a) Location (dashed frame) of the study area in SRTM background image. Inset: Arabia-Eurasia collision zone with the GPS-derived velocity for the northern margin of the Arabian plate (18 ± 2 mm yr^{-1}) relative to Eurasia (Ghalamghash et al.,2016), QDF: Qoshadagh Fault, NKF: Nakhchivan Fault. (b) QDF fault on SRTM relief map.

STRUCTURES

Mapping of the August 11, 2012 rupture of the QDF revealed that there are at least one or more poorly known or unknown fault zone(s) that actively accommodate the transpressional deformation in NW Iran (Copley et al., 2013 ; Faridi et al., 2017 ; Faridi & Sartibi, 2012). The more than 150 km long, dominantly right-lateral QDF extends from southwest of Varzegan City (*Figure 1*) to the southeastern flanks of the Sabalan Volcano (*Figure 1b*). The map pattern shows three segments. The central, roughly E–W striking segment, bounds the northern flank of the Qoshadagh Mountain Range (*Figure 1b)*. To the east, the Qoshadagh Mountain Range terminates with the semi-active Sabalan Plio-Quaternary Volcano (*Figure 1b*), where the QDF strike turns clockwise to form the NW–SE striking eastern segment of the fault. This new orientation forms a releasing bend with several splay faults across the Mount Sabalan (*Figure 1b*). Transtension in this eastern splay array has played an important role in the evolution of the Plio-Quaternary Sabalan Volcano (Faridi, 2010). The western QDF segment is another set of NW–SE striking splay faults to the Southwest of Varzegan City (*Figure 1b*). Satellite images and remote sensing data show continuity of the western segment with the NW–SE striking Nakhchivan active Fault (NKF), further northwest, beyond Jolfa City (*Figure 1a*).

SEGMENTS OF THE QOSHADAGH FAULT

Central Segment

The central segment is the longest, about 100 km (*Figure 1b*), with a general strike of E–W, delineates the northern boundary of the Qoshadagh Mountain Range (*Figure 1b*), a prominent morphotectonic feature that reaches 2980 m asl. Field surveys and measurements of kinematic indicators on fault planes indisputably indicate dominant dextral movement accompanied by a small reverse component (*Figure 2a*). In several places, the fault cuts through Quaternary alluvium and has deflected rivers and streams (*Figure 3* , *Figure 4*). The surface rupture (*Figure 5* , *Figure 6*) and the focal mechanism of the August 11, 2012 event (Faridi & Satribi, 2012 ; Ghods et al., 2015) are both consistent with the dextral-reverse movement.

Eastern Segment

The NW–SE striking splay faults form a large-scale transtensional horsetail pattern (*Figure 7*) cutting through Quaternary lava flows of Mount Sabalan (*Figure 7c*). The Moil valley fill sediments and lahar deposits have recorded syn-depositional normal faulting and extensional soft-sediment structures (Faridi, 2010). The extensional component of the splay fault pattern may have facilitated upper crustal magma migration and installation of the Sabalan Volcano. The Alvars splay fault (*Figure 7b*) may extend further southeast toward the

Owjur Village (*Figure 1b*) in foothills of Mount Sabalan where the epicenter of the destructive February 28, 1997 Ardabil earthquake is located (Faridi et al., 2017 ; Zare, 1997). The southwestern flank of the Sabalan edifice has been destabilized and collapsed in consistency with the transtensional movements (*Figure 7d*).

Western Segment

The Qaraqaya Valley (*Figure 1b*) is a morphotectonic feature corresponding to one of the fault splays of the QDF western segments. It separates Cretaceous turbidites in the southeastern fault block from Plio-Quaternary volcanoclastics to the northeast. Faults have displaced Plio-Pleistocene volcanoclastic layers and offset drainage and streams to the north of Brundara Village (*Figure 1b*). Kinematic indicators on the exposed fault planes confirm dextral- normal slip (*Figure 2d, f*).

MORPHOTECTONIC FEATURES

We measured various amounts of horizontal and vertical geomorphic offsets along the 15 km long surface rupture of the 2012 earthquake. Some geomorphic features have actually been displaced by multiple earthquakes and the measured offsets represent cumulative amounts of surface movements. We used kinematic GPS (Real Time Kinematic/GNSS) during the fault surveys to obtain precise measurements. The resulting values were used for calculation of fault parameters and preparation of digital elevation models.

We separated the 2012 displacement from the older offsets, using displacement across manmade linear features like grooves in plowed lands, farms boundaries, irrigation channels, roads and motor-able tracks as well as slightly incised lands and narrow gullies. During the 2012 event, the maximum horizontal and vertical displacements were 1.0 and 0.3 m, respectively.

The largest cumulative displacement measured along the ruptured strand of the QDF is 160 ± 5 m, the offset of the mountain front to the north of Chobanlar Village (*Figure 6, Figure 8b*). To the northwest of Chobanlar Village (*Figure 8c, d*), RTK GPS surveys of deflected gullies yield a horizontal offset of 2.23 ± 0.1 m only 0.8 m of which are due to the 2012 earthquake (see section“T3-EII”Event). The results of the kinematic GPS survey also indicate a 0.97 ± 0.1 m vertical uplift of the northern (hangingwall) block with 0.3 m due to the 2012 event. Further west, near the western end of the central segment, the Sarandchay River Valley (*Figure 6*) has undergone a 64 ± 1 m offset (*Figure 9*). Along the strand of the 2012 rupture, the river channel and adjacent young alluvial strath terraces are dextrally offset by 4.5 ± 0.5 m (*Figure 9b*). The displacement magnitude and location measured and calculated using geomorphic features, are given in *Table 1*.

PALEOSEISMOLOGY

In order to specify the geometrical and seismic parameters of the QDF central segment, three trenches

(QDF-T1 to T3) were excavated across the surface rupture of the August 11, 2012 earthquake. High level underground water and soil disturbance during agricultural activity led us to select trenching sites at the eastern end of the surface rupture, north of Chobanlar Village. The trenches were excavated nearly orthogonal to the E–W strike direction of the rupture (*Table 2*).

The three trenches excavated Pliocene-Pleistocene (Faridi & Haghfarshi, 2006) bed rocks and their overlying, unconsolidated sedimentary cover displaced by faults. Some of the faults were restricted to the bed rocks with their tips terminating against the unconformity of the overlying Quaternary sediments, in which various paleosurfaces constrain the relative timing of paleoearthquake events.

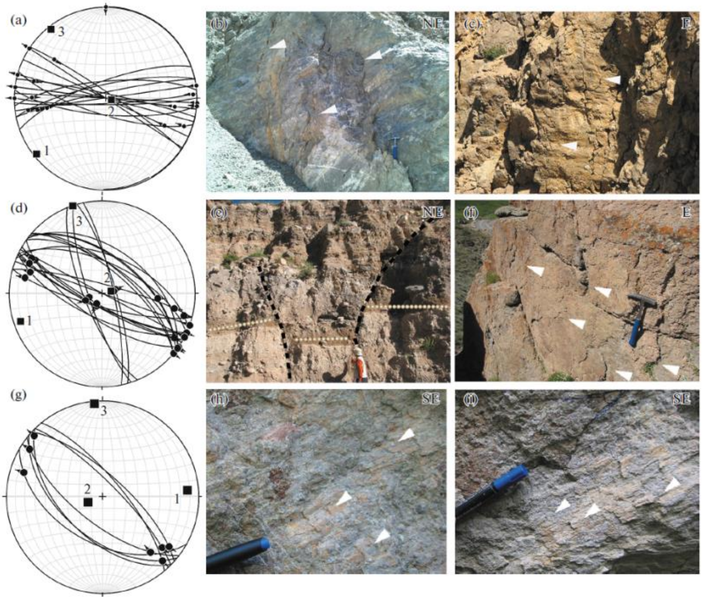

Figure 2: Comparison of attitude and slip directions of fault planes exposed along the QDF segments. Stereographic diagrams (a, d and g): equal-area, lower hemisphere projection (generated with Fault-Kin-Win) (Allen et al., 2013) of measured fault planes along the central, western and eastern segments of the QDF respectively, documenting the prominent right-lateral sense of slip. Fault plane (great circle), slickenline pointing to the direction of movement of the hangingwall (arrows), kinematic (squares) axes: (1) contraction, (2) intermediate, (3) extension. (b) Dextral fault plane exposed to the northeast of Chobanlar Village, attitude of fault plane: 087/82S, slickenside lineations: 15/278. (c) Dextral fault plane exposed to the southeast of Goradara Village, attitude of fault plane: 093/90, slickenside lineations: 05/093. (e) Normal faults in volcanoclastic layers exposed on northwest of Moil Village. (f) Dextral fault in volcanoclastic

sediments of Mount Sabalan, Riedel shear joints indicate dextral movement. (h) Dextral-normal fault in volcanoclastic sediments exposed on Qaraqaya road-cut. (i) Slickenside on a splay fault of western segment, north of Brundara Village. Calcite fibers used as shear sense indicators demonstrate dextral-normal movement. Fault attitude: 135/67 SW, lineations: 25/145.

Trench QDF-T1

The paleoseismic QDF-T1 trench site is located to the northeast of Chobanlar Village (*Figure 6*). The structural features of the trench are summarized in *Table 2*.

Sedimentary succession

The western wall of the trench exposes an upward fanning, positive flower structure. The total displacement is partitioned among five steeply dipping to vertical fault planes (*Figure 10a*). F4 (087/75N) is the youngest, and has breached the top soil during the August 11, 2011 Varzegan-Ahar earthquake. This fault plane divides the investigated trench into two sedi-mentologically distinct blocks (*Table 3*). The northern, hangingwall block, mainly consists of up-raised Plio-Pleistocene stratified tuff, volcanic breccia and volcanoclastic conglomerate (*Figure 10*, U1 and U2). These pyroclastics are overlain by Holocene alluvial sedimentary sequences (*Figure 10*, U3, U6, U7 and U8). The footwall block consists of volcanoclastics confined to the bottom of the trench and covered by loose and poorly consolidated Holocene alluvial sediments (*Figure 10*, U4 to U8). Radiocarbon dating of the detrital samples taken from the base of the oldest sedimentary unit (*Figure 10*, U3) yielded ages not older than 2058 *Figure 10a*, Maximum age of sample T1-OC2 from U3: 41 Cal BC). A calibrated calendar youngest age obtained from sample T1-OC1 from U7, which is breached by both most recent and penultimate earthquakes, is 1517 Cal AD ± 126 yr.

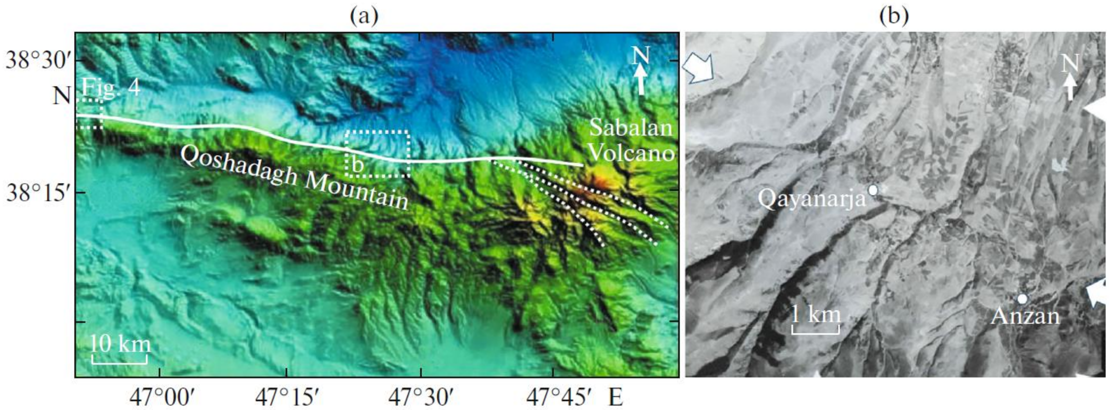

Figure 3: Right lateral deflection and offset of streams along the QDF central segment. Northern flank of Qoshadagh, Northwest of Anzan Village.

Figure 4: Right lateral offset of the drainage pattern along the QDF central segment. Northern flanks of Qoshadagh, east of Goradara Village.

Figure 5: Surface rupture due to the 2012 earthquake on the QDF central segment. (a) pressure ridges formed in left-stepping rupture segments, circled: hammer for scale. (b) dextral-reverse rupture of the Varzegan-Tabriz Road on the left bank of Sarandchay River.

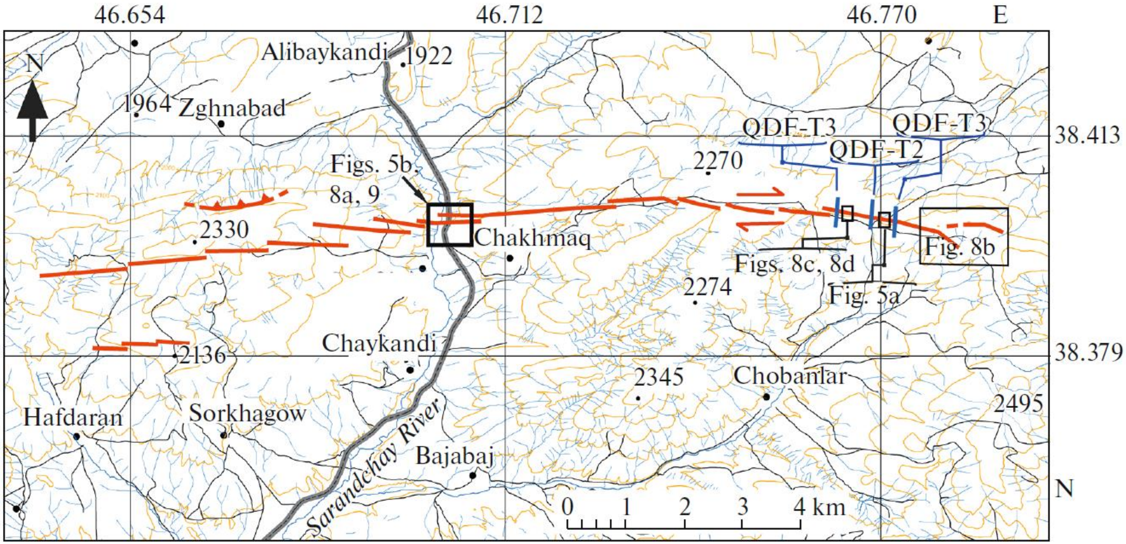

Figure 6: Surface rupture map of the 2012 earthquake (Faridi et al., 2010) and location of excavated trenches.

Identification of past earthquake events

According to the structural and sedimentary observations, retro-deformational sequence (*Figure 10*, restoration of trench log) and results of calibrated radiocarbon dating, the western wall of QDF–T1 trench provides evidence for at least four surface rupturing earthquakes along the F4 and F5 faults.

T1-EI (*Figure 10a*) is the dextral-reverse August 11, 2012 event that displaced U2, U6, U7 and U8 along F4. The vertical separation (V) is 25 ± 1 cm. To the west, 100 m from the trench QDF-T1, along the surface rupture, displaced manmade water channels, field boundaries and geomorphic and landform offsets (*Table 1*) indicate a maximum horizontal separation (H) of 75 ± 5 cm.

T1-EII (*Figure 10b*) event corresponds to a historical (1567 AD) earthquake (Zoka, 1989). In retro-deformation to pre-T1-E1 stage, the thickness of both U7 and U6 are different on the two sides of F4. The youngest unit of U7, dated at 1517 Cal AD ± 126 yr, has undergone 15 ± 1 cm reverse component which according to the average 20°W pitch of striations, implies 47 ± 1 cm horizontal separation. According to the geometric characteristics of the fault and assuming a rigidity module of 3×10^{11} (dyne/cm^2) and using the empirical equation that relates fault rupture area with moment magnitude (*Table 4*) and (Wells & Coppersmith, 1994), the calculation yields a magnitude of Mw ≈ 6.3 for T1-EII.

T1-EIII. A relatively large age difference (≈735 years) between sedimentary units U7 and the underlying U6 reveals a local sedimentation gap or erosion which has wiped out at least one surface rupture event, according to correlations with the other trenches. The base of U7 seals the F4 fault, which has breached U6 with a radiocarbon age of 781 Cal AD ± 113 yr (*Figure 10c*). Using the fault characteristics (*Table 4*) and applying the same earthquake magnitude calculation as for T1-EII, the moment magnitude of T1-EIII was Mw ≈ 6.4.

T1-EIV. This event is identified from F5 cutting U4 dated at 185 Cal AD ± 55 yr and sealed by the 781 Cal AD ± 113 yr U6. Using the fault slip parameters (*Table 4*) and assuming an inferred average focal depth of 12 km (Ghos et al., 2015), we obtained a magnitude of Mw ≈ 6.2. F1, F2 and F3 faults breach the Plio-Pleistocene bed rocks (*Figure 10d*) and do not provide information on earthquakes older than U3 (41Cal BC).

Trench QDF-T2

The trench QDF-T2 was excavated 200 m to the west of QDF-T1 (*Figure 6*). A summarized description is given in *Table 2*.

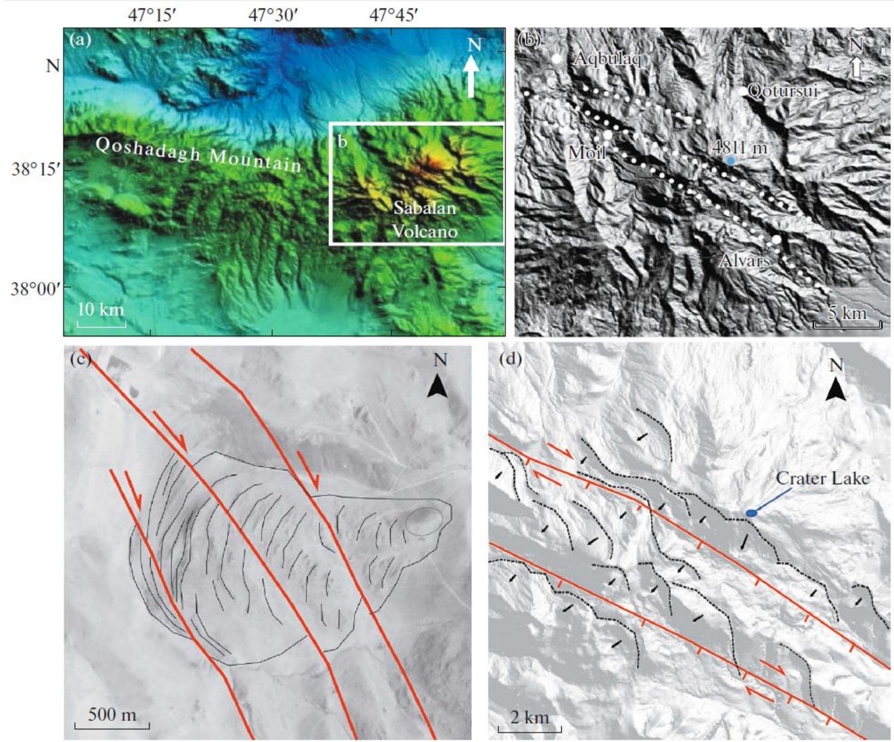
47°15′
47°30′
47°45′
N
38°15′
38°00′
(a)
N
Qoshadagh Mountain
b
Sabalan Volcano
10 km
(b)
Aqbulaq
N
Qotursui
Moil
4811 m
Alvars
5 km
(c)
N
500 m
(d)
N
Crater Lake
2 km

Figure 7: (a) Horsetail splays forming the western segment of QDF breaching the Mount Sabalan caldera walls (Faridi & Sartibi, 2012). (b) DEM presented as a hill shade map (sun elevation = 45°, Azimuth = 045°) shows the Mount Sabalan edifice breached and collapsed by NW–SE striking dextral-normal faults. (c) Young (post-caldera) lava flows displaced by a set of dextral-normal faults to the east of Moil Village. (d) Southwestern flank of the Sabalan edifice destabilized and collapsed by the transtensional movements. Escarpments of gravitational slides and rock avalanches, are restricted to the SW facing fault escarpments.

Sedimentary succession

The eastern wall of the trench exposes a 1 m wide, upward fanning, and negative flower structure. There are three sub-vertical branches (*Figure 11*, F1 to F3). F2 (fault plane attitude: 087/75N) has breached the top soil during the August 11, 2012 earthquake (*Table 5*).

Right-stepping segments of the dominantly dextral rupture of the August 11, 2012 surface rupture in trench QDF-T2 produced small depressions of the land surface, which reflect normal components of the fault planes. The trench is divided by F2 into two sedimentologically distinct parts. Pliocene-Pleistocene volcanoclastic breccia, tuff and ash layers are exposed all along the bottom of QDF-T2. Holocene sediments overlying the volcanoclastic bedrocks have different sedimentological characteristics (color, texture, packing and composition of grains) in the hangingwall and footwall of F2 (*Figure 11*, *Table 5*). The Holocene sediments were accumulated in the fault-related small depressions and are dominantly derived from erosion of nearby, relative highlands. There are evident similarities with rocks and sedimentary units exposed in the other two trenches. OSL samples from QDF-T2 contain an inherited amount of luminescence dose and therefore yield overestimated ages due to both the close distance to the provenance and partial solar resetting before burial. In order to get an age estimate, we made extrapolation based on sedimentological and deformational characteristics of sedimentary units dated in QDF-T1 and QDF-T3 (*Figure 12*).

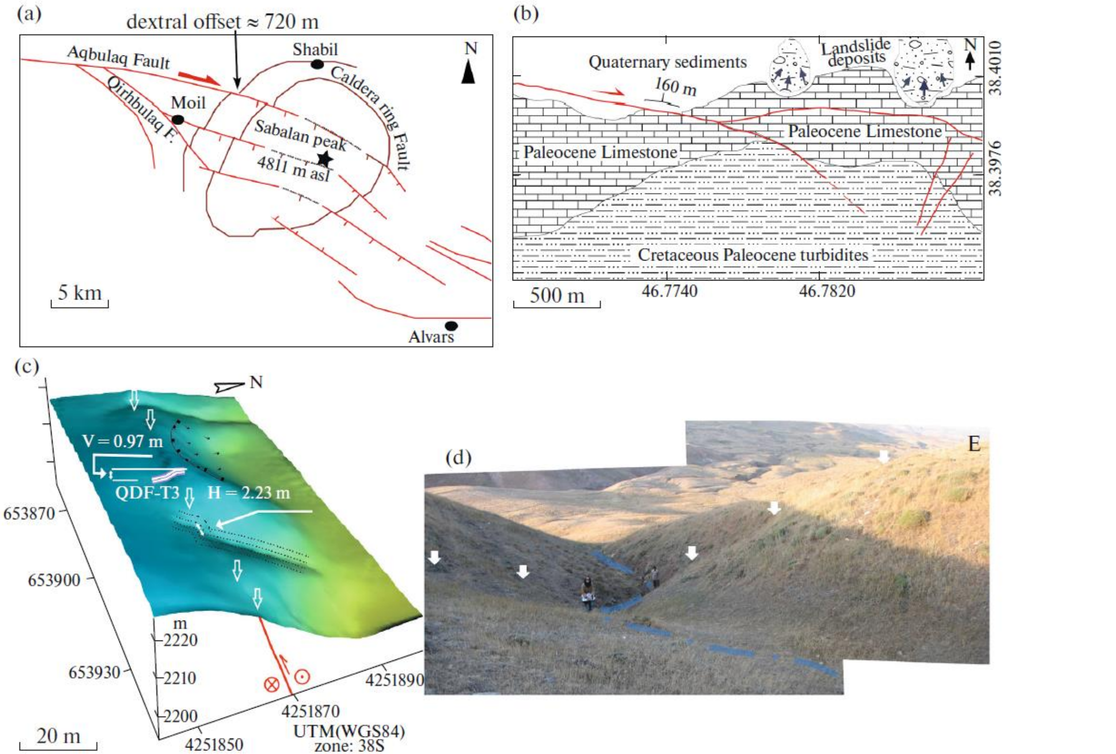
(a)
dextral offset ≈ 720 m
Aqbulaq Fault
Shabil
Caldera ring Fault
Qirhbulaq F.
Moil
Sabalan peak
4811 m asl
N
5 km
Alvars
(b)
Quaternary sediments
Landslide deposits
160 m
Paleocene Limestone
Paleocene Limestone
Cretaceous Paleocene turbidites
N
38.4010
38.3976
500 m
46.7740
46.7820
(c)
N
V = 0.97 m
QDF-T3
H = 2.23 m
653870
653900
653930
m
2220
2210
2200
20 m
4251850
4251870
4251890
UTM(WGS84)
zone: 38S
(d)
E

Figure 8: Cumulative offsets measured along the QDF. (a) Sabalan caldera dextrally displaced by 720 m. (b) 160 m dextral displacement of Qoshadagh Mountain front, northwest of Chobanlar Village. (c) DEM resulted from RTK surveys on offset drainage east of paleoseismic trench QDF-T3, shows the cumulative 2.23 m dextral drainage offset and 0.97 m uplift of hangingwall. (d) Dextral- reverse drainage offset.

Past earthquake events

QDF-T2 trench has recorded at least three paleoearthquakes over the past 1200 years. Besides the 2012 earthquake (*Figure 11a*), the identified penulti-mate event (*Figure 11c*) corresponds probably to the historical 1567 AD earthquakes in Azerbaijan Region (Zoka, 1989), if correlations with QDF T1 and T3 are valid. U6 and U3 predate and postdate the oldest event (*Figure 11d*) and bracket its age between 781 Cal AD ± 113 and 1517 Cal AD ± 126 yrs. The fault slip parameters and calculated moment magnitudes for each paleoearthquakes are given in *Table 4*.

Trench QDF-T3

The paleoseismic trench QDF-T3 (*Table 2*) was excavated 550 and 750 m to the west of QDF-T2 and QDF-T1, respectively.

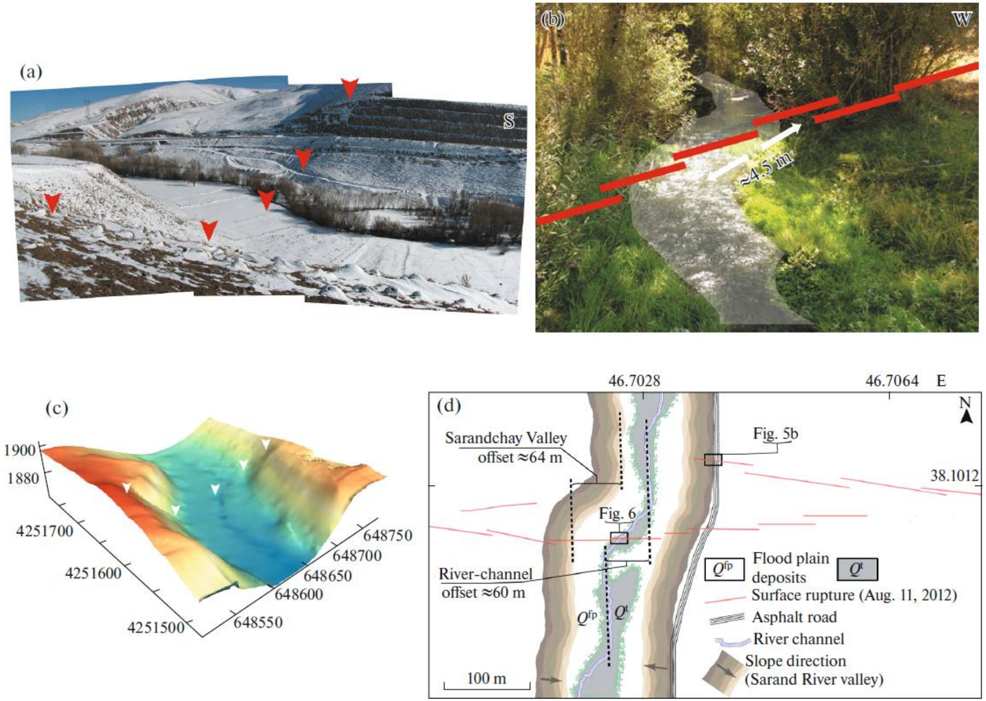
(a)
S
(b)
W
≈4.5 m
(c)
1900
1880
4251700
4251600
4251500
648750
648700
648650
648600
648550
46.7028
46.7064 E
(d)
N
Sarandchay Valley
offset ≈64 m
Fig. 5b
38.1012
Fig. 6
River-channel
offset ≈60 m
Q^{fp}
Q^{t}
Flood plain
deposits
Surface rupture (Aug. 11, 2012)
Asphalt road
River channel
Slope direction
(Sarand River valley)
100 m

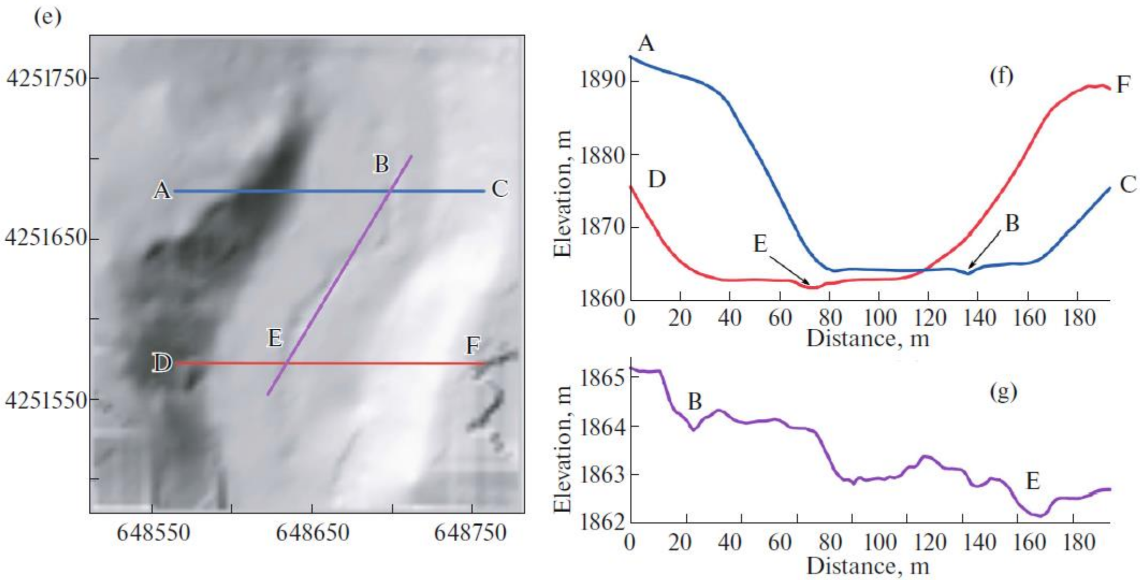

Figure 9: Cumulative offset of Sarandchay River. (a) Dextral deflection along the River Valley, arrows indicate QDF trace. (b) The modern river channel offset by 4.5 m along the ruptured strand of the QDF. (c) DEM resulted from RTK survey along the river valley. (d) Sketch image shows amount

of the offsets and position of related photos. (e) Profile lines of A–C (blue) and DF (red) are parallel to the QDF and BE (violet) along the deflected stream. (f) Profiles demonstrate precise amount of 64 ± 1 m horizontal displacement across the river-valley and E and B as piercing points indicate a right-lateral offset of 60 ± 1 m in a 150 m wide fault zone. (g) Profile showing the 2 m elevation contrast between the two sides (hangingwall and footwall) of the recent surface rupture.

Stratigraphy and structure

The eastern wall of QDF-T3 (*Figure 13a*) is characterized by a 6 m wide fault zone with nine, steeply north-dipping dextral-reverse fault planes (*Figure 13*, F1 to F8).

F4, F5 and F6 faults have breached the top soil (U5) during the 2012 surface rupture. F6 is the major plane between the northern and southern blocks. The northern block is the up-raised hangingwall, which mainly consists of Pliocene-Pleistocene volcanoclastic sediments (U1) covered by thin (≈0.3 m) detrital Holocene deposits. The Plio-Quaternary bedrock in the footwall block consists of volcanic ash and tuff (U2) overlain by relatively thick sedimentary units including an imbricated colluvial wedge (U3). The wedge shaped chaotic and poorly sorted colluvium was sourced from erosion of the F6 paleo-escarpment. To the south, F7, F8 and F9 breached U3 and U4 during later paleoearthquakes.

Table 1: Field records and calculated fault parameters on surface rupture of recent (2012) earthquake on QDF

Point	Position latitude/ longitude	Feature	Recent horizontal offset	Recent vertical offset	Dip slip, cm	Net slip, cm	Cumulative offset	Pitch or rake, W
Rptmx	38.4017 46.7582	Drainage Offset	95 cm/dextral	25 cm/reverse	27	_	_	17°
Rupture3 (west of T3)	38.4017 46.7624	Drainage Offset	75 cm/dextral	30 cm/reverse	32	99	_	24°
Gpskin (east of T3)	38.4018 46.7626	Drainage Offset	75 cm/dextral	27 cm/reverse	29	_	2.25 m dextral	20°
Guardrailrupt	38.4015 46.7037	Displaced main road	55 cm/dextral	20 cm/reverse	21	82	_	19°
Rpt4rio	38.4003 46.7022	Sarand River Channel offset	65 cm/dextral	20 cm/reverse	21	_	4.5 m dextral	16°
Rpt4rio-b	38.4003 46.7022	Sarand River Valley offset	65 cm/dextral	20 cm/reverse	21	_	64 m dextral	16°
Rupt33	38.4025 46.7250	Farms boundary offset	70 cm/dextral	15 cm/reverse	16	80	_	14°
Rupt26	38.4027 46.7293	Displaced road	75 cm/dextral	25 cm/reverse	27	59	_	20°
Rupt21	38.4038 46.7341	Farms boundary offset	73 cm/dextral	25 cm/reverse	27	68	_	20°
Rupt8	38.4010 46.7691	Farm boundary offset	80 cm/dextral	10 cm/normal	11	72	_	10°
Rupt8b	38.4009 46.7693	Farm water supply offset	80 cm/dextral	10 cm/normal	11	72	_	10°
Ruptprg	38.4018 46.7600	Pressure ridge	75 cm/dextral	30 cm/reverse	32	80	_	24°
Rpt16	38.3987 46.7797	Displaced farm grooves	75 cm/dextral	25 cm/reverse	27	78	_	19°
Rptmount	38.3998 46.7746	Obliquely displaced mountain front	75 cm/dextral	20 cm/reverse	21	81	160 m dextral	20°

Table 2: Position and geometric characteristics of the excavated trenches on QDF

Trench ID	Latitude	Longitude	Elevation	Length	Depth	Trend	Investigated wall	Apparent structure
QDF- T1	38.401 N	46.771 E	2181 asl	7 m	3 m	N–S	West wall	Positive flower
QDF- T2	38.401 N	46.769 E	2211 asl	7 m	3 m	N–S	East wall	Negative flower
QDF- T3	38.4017 N	46.762 E	2219 asl	10 m	3 m	N–S	East wall	Imbricated

Past earthquakes

Structural and sedimentary records in QDF–T3 provide evidence for at least three surface rupturing paleoearthquakes.

T3-EI. The youngest T3-EI (*Figure 13a*) is the August 11, 2012 event, which has breached the top soil. The corresponding F4, F5 and F6 fault branches cut all rock units with dextral-reverse displacement. F5 and F6 show only the reverse component (total vertical displacement = 28 ± 2 cm). En echelon fissures at the top of F4 correspond to a nearly pure dextral surface rupture of 75 ± 5 cm and imply that the coseismic fault slip was partitioned as pure reverse on F5 and F6 and pure dextral on F4.

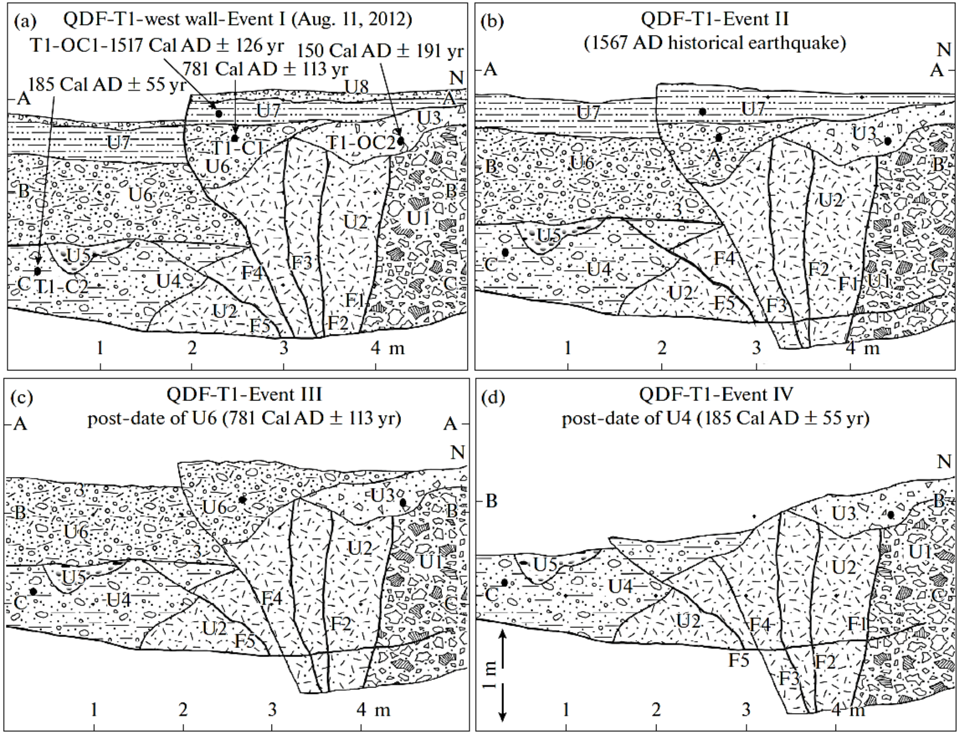
(a) QDF-T1-west wall-Event I (Aug. 11, 2012)
T1-OC1-1517 Cal AD ± 126 yr
150 Cal AD ± 191 yr
781 Cal AD ± 113 yr
185 Cal AD ± 55 yr
T1-C1
T1-OC2
T1-C2
(b) QDF-T1-Event II
(1567 AD historical earthquake)
(c) QDF-T1-Event III
post-date of U6 (781 Cal AD ± 113 yr)
(d) QDF-T1-Event IV
post-date of U4 (185 Cal AD ± 55 yr)
U1
U2
U3
U4
U5
U6
U7
U8
F1
F2
F3
F4
F5
A
B
C
N
1
2
3
4 m
1 m

Figure 10: (a) Profile of the western wall of trench QDF-T1 displaying rocks and sedimentary units (U1 to U8) displaced by fault branches (F1 to F5). Sampling sites and resulted radiocarbon age of the units are given in AD calendar. A, B and C intervals (in vertical axis) is 1 m. (b, c, d) Retro-deformational sequence of the past earthquakes in QDF-T1. Bed rocks accompanied with overlying sedimentary units restored, in 4 steps, into their successive stages to measure horizontal and vertical displacements.

T3-EII. After restoration (*Figure 13a, b*) most faults terminate at the base of U5. Beneath this unconformity, U4 and older units are cut and displaced by multiple fault splays. The thickness of displaced U4 blocks varies from block to block, which indicates that the deformed ground surface and fault escarpment created by previous earthquake events were flattened by erosion before deposition of U5. Retro-deformation (*Figure 13b*) shows that F2, F6, F7, F8 and F9 have contributed to the ground deformation and sliced U3 and U4. The total T3-E 2 vertical separation of U4 is 50 ± 10 cm which, considering the average 20°W pitch of striations, results in strike slip separation of 137 ± 10 cm. This estimate is consistent with the horizontal offset of a small gully next to QDF-T3 (*Figure 8c, d*). Radiocarbon ages of breached U4 and sealing U5 bracket T3-EII between 1562 Cal AD ± 121 and 1799 Cal AD ± 126 yrs. The age range includes the historically reported 1567 destructive earthquake (Trifonov, 1995). Using the fault plane parameters (*Table 4*) and the same equation linking them to earthquake magnitude (Wells & Coppersmith, 1994), yields Mw ≈ 6.7.

Table 3: Description of sedimentary unis and underlying bed rocks exposed in QDF-T1

Unit	Fault block	QDF-T1 Units descriptions
U8	HW and FW	Gravely and sandy mud, brown colored, porous top soil with plant remains (roots and stems)
U7	HW and FW	Moderately compact, dark grey gravely mud, with organic materials. Pebbles floating within fine, plastic soil matrix. (^{14}C age: 1391–1643 Cal AD)
U6	HW and FW	Inhomogeneous, chaotic (non-stratified) dark brown, matrix-supported gravely clay. Uniform composition and sub-angular cobble and pebbles of grains indicating small and proximal source area. (^{14}C age: 668–894 Cal AD)
U5	FW	Gravely mud, stratified, channel fill deposits, oriented pebbles indicating northward flow direction
U4	FW	Inhomogeneous, poorly-sorted, dark brown to black polymodal gravely clay with pebble-sized (up to 4 cm) sub-angular to sub-rounded grains, largely sourced from nearby loosened and eroded limestone and volcanoclastic outcrops (^{14}C age: 130–240 Cal AD)
U3	HW	Inhomogeneous, grey colored, poorly-sorted, non-stratified and unimodal gravely sand with reworked sub-angular clasts mostly derived from disintegrated volcanoclastic rocks. Erosional products of U1, Fine particles washed away. (^{14}C age: 41Cal BC–340Cal AD)
U2	HW and FW	Bed rock 2, acidic fine grained tuff and ash layers, weathered and kaolinitized, red ferruginous tuff strata (Plio-Quaternary bed rock subjected to erosional processes)
U1	HW	Bed rock 1, Volcanoclastic breccia and conglomerate, coarse grains embedded in tile red stratified tuffaceous matrix, attributed to Plio-Quaternary volcanism

T3-EIII. The base of the U3 colluvium wedge seals F6 (*Figure 13b, c*). This is evidence for the "T3-EIII"event being timely close in age to deposition of U3 (1346 Cal AD ± 88 yrs). Restoration (*Figure 13c*) shows 68 ± 5 cm vertical separation for U1 and U2 along the F2 and F6 faults. With the average 20°W pitch of net slip vector brings in 186 ± 5 cm horizontal offset. The calculated moment magnitude is Mw ≈ 7.0 (*Table 4*, *Table 6*).

Table 4: Geometrical parameters and obtained seismic parameters of the QDF-T1, T2 and T3

Trench	Event ID	Event sequence	Event horizon	Displaced units	Age ± 2σ (Cal AD)	Ds, m	V, m	Ss, m	Sn, m	Pitch, deg	L, km	F, km	A, km^2	M_0^g, dyne cm	M_w
QDF. T_1	T1-E_I	MRE	Recent land surface	U2, U6, U7 and U8	11/Aug/2012	0.27	0.25	0.75	0.80	20 W	14	12	168	4.03^{25}	6.37
	T1-E_{II}	PE	Base of unit 8	U2, U4, U6 and U7	Post-date of U 7 (1517 Cal AD ± 125 yr)	0.16	0.15	0.47	0.50	20	20	12	240	3.6^{25}	6.33
	Hiatus	–	–	–	–	–	–	–	–	–	–	–	–	–	–
	T1-E_{III}	AAPE	Base of unit 7	U2 and U6	Post-date of U6 (781 Cal AD ± 113 yr)	0.27	0.25	0.75	0.80	20	14	12	168	4.03^{25}	6.37
	T1-E_{IV}		Base of unit 6	U2 and U4	Post-date of U4 (185 Cal AD ± 55 yr)	0.16	0.16	0.44	0.47	20	12	12	144	2.03^{25}	6.17
	T1-E_V		Base of unit 3	U1 and U2	Pre-date of U3 (150 Cal AD ± 191 yr)	?	?	?	?	?	?	12	?	?	?
QDF. T_2	T2-E_I	MRE	Recent land surface	U2, U4, U5, U6 and U7	11/Aug/2012	0.11	0.10	0.75	0.76	7	14	12	168	3.85^{25}	6.35
	T2-E_{II}	PE	Base of unit 7	U2, U4, U5 and U6	Post-date of U6 (1537 Cal AD ± 146 yr)	0.13	0.12	0.74	0.75	9	20	12	240	5.4^{25}	6.45
	T2_E_{III}	APE	Base of unit 6	U1, U2, U3, U4 and U5	Pre-date of U6 (1537 Cal AD ± 146 yr)	0.18	0.17	0.74	0.76	13	25	12	300	6.84^{25}	6.52
QDF. T_3	T3-E_I	MRE	Recent land surface	All units	11/Aug/2012	0.30	0.28	0.75	0.81	22	14	12	168	4.08^{25}	6.37
	T3-E_{II}	PE	Base of unit 5	U1, U2, U3 and U4	Post-date of U4 and pre-date of U5 (1562 Cal AD ± 120 yr)–(1798 Cal AD ± 158 yr)	0.53	0.50	1.37	1.46	20	25	≤15	300	1.314^{26}	6.71
	T3-E_{III}	APE	Base of units 3 and 4	U1 and U2	Most close to date of U3 (Max. age: 1346 Cal AD ± 88 yr)	0.72	0.68	186	198.88	20	30	≤15	300	3.6^{26}	7.00

The quantities derived from measurements on three trenches and their restored logs. V means vertical separation; Ds, dip slip = ($V.Sin^{-1}\ \delta$); Ss, strike slip; Sn, net slip = $(Ds^2 + Ss^2)^{0.5}$; Pitch or rake equals Arc Cos (Ss/Sn); L, rupture length; D, focal depth; A, rupture Area = L × F; Mw, energy magnitude or moment magnitude (Hanks & Kanamoi, 1979) that equals 2/3 Log M_0^g – 10.7, where M_0^g is the seismic or geologic moment (Aki & Richards, 1980) that equals μ × A × Sn, and here μ is the shear or rigidity module = 3×10^{11} (dyne/cm^2). E.g., $M_0^g = 3 \times 10^{11}$ (dyne/cm^2) × (14.5×10^5 (cm) × 12×10^5 (cm) × 0.80×10^2 (cm) = 3.93×10^{25} (dyne cm); Mw = 2/3Log3.93×10^{25} – 10.7 = 6.4.

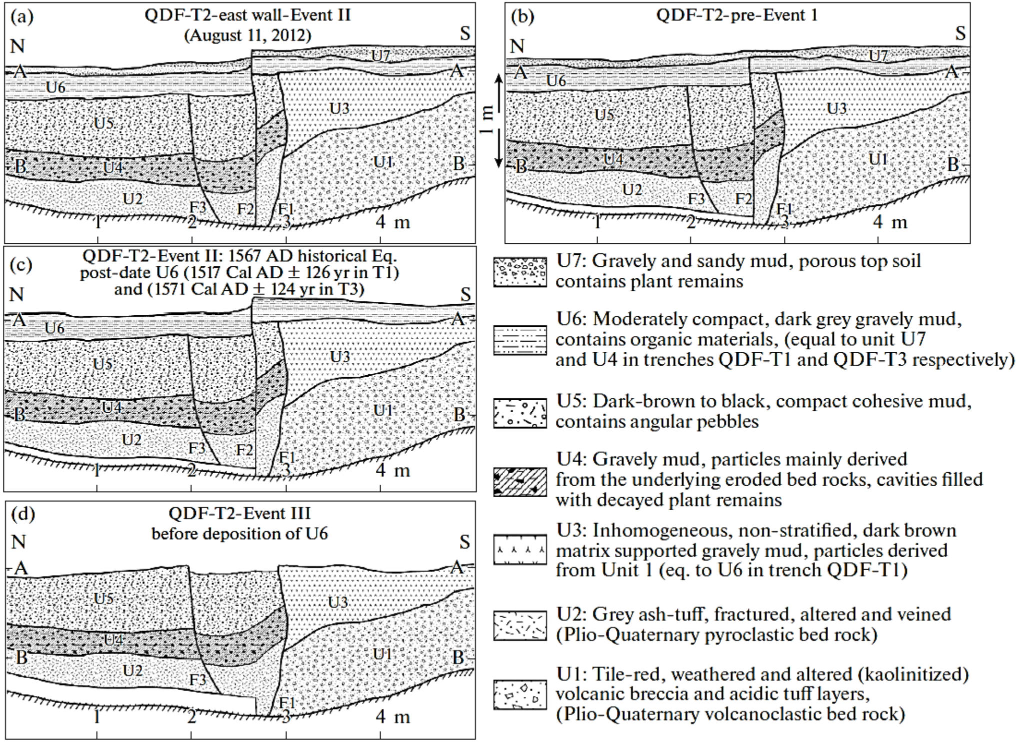
(a)
QDF-T2-east wall-Event II
(August 11, 2012)
(b)
QDF-T2-pre-Event 1
(c)
QDF-T2-Event II: 1567 AD historical Eq.
post-date U6 (1517 Cal AD ± 126 yr in T1)
and (1571 Cal AD ± 124 yr in T3)
(d)
QDF-T2-Event III
before deposition of U6
N
S
A
B
U1
U2
U3
U4
U5
U6
U7
F1
F2
F3
1 m
1
2
3
4 m
U7: Gravely and sandy mud, porous top soil contains plant remains
U6: Moderately compact, dark grey gravely mud, contains organic materials, (equal to unit U7 and U4 in trenches QDF-T1 and QDF-T3 respectively)
U5: Dark-brown to black, compact cohesive mud, contains angular pebbles
U4: Gravely mud, particles mainly derived from the underlying eroded bed rocks, cavities filled with decayed plant remains
U3: Inhomogeneous, non-stratified, dark brown matrix supported gravely mud, particles derived from Unit 1 (eq. to U6 in trench QDF-T1)
U2: Grey ash-tuff, fractured, altered and veined (Plio-Quaternary pyroclastic bed rock)
U1: Tile-red, weathered and altered (kaolinitized) volcanic breccia and acidic tuff layers, (Plio-Quaternary volcanoclastic bed rock)

Figure 11: (a) Profile of QDF-T2, showing sedimentary units (U1 to U7) displaced by fault planes (F1 to F3). Correlated sedimentary units combined with results of radiocarbon age of the equivalent units are indicated. (b, c, d) Retro deformational sequence of QDF-T2. Bed rocks and overlying sedimentary units restored in successive pre-event stages to measure respective vertical displacements and estimate horizontal offsets.

Average Slip Rate Estimates

We used ages of differently elevated strath terraces in the Sarandchay River (*Figure 9*) to estimate the Late Holocene slip rate along the QDF central segment. The OSL age of sample (*Table 7*, QDF-t1-OSL1), from the 4.5 ± 0.5 m dextrally offset terrace immediately above the river channel, is 2.61 ± 0.31 ka. It allows calculating a mean slip rate of 1.7 ± 0.3 mm yr^{-1} for the past 3 ka. OSL Dating of another sample taken from an older, higher alluvial terrace (QDF-t1-OSL2) on the left bank of the Sarandchay River, yields a minimum age of 75 ka which, according to the 64 m offset of the valley (*Figure 9*), gives an average slip rate of 0.9 mm yr^{-1}. Paleoseismic trenches have provided data for the last ≈2.5 ka, yielding an average slip rate of 1.9 ± 0.1 mm yr^{-1}. The rate of vertical component is 0.7 ± 0.1 mm yr^{-1}. Taking 70°N the average dip of the QDF plane, the average N-S shortening rate across the fault is 0.3 ± 0.1 mm yr^{-1}. To the northwest of the Sabalan Volcano, in the eastern segment of the QDF, the NW-striking fault splay has displaced dextrally the caldera wall by 720 ± 25 m (*Figure 8a*) (Faridi, 2010). The published 545 ± 40 ka U–Pb zircon age of ignimbrites associated with the collapse of the caldera (Ghalamghash et al., 2016) allows calculating an average slip rate of 1.4 ± 0.2 mm yr^{-1} over the past 500 ka. Comparison of the different values of the relatively short-term and long-term slip rates imply that the QDF has increased its mean slip rate over the past few millennia.

Table 5: Description of sedimentary unis and underlying bed rocks exposed in QDF-T2

Unit	Fault block	QDF-T2-Descriptions
U7	Northern and Southern blocks	Gravely and sandy mud, brown colored, porous top soil with plant remains (roots and stems). Equivalent to U8 in QDF-T1 and U5 in QDF-T3 (^{14}C ages: min. 1652—max. 1955 Cal AD)
U6	Northern and Southern blocks	Moderately compact, dark grey gravely mud with organic matter. Pebbles floating within fine soil matrix. Equivalent to U7 in QDF-T1 and U4 in QDF-T3 (^{14}C ages: min. 1391—max. 1683 Cal AD)
U5	Northern block	Dark-brown to black, compact cohesive mud containing angular pebbles
U4	Northern block	Gravely mud with particles mainly derived from the underlying eroded bed rocks, Organic rich cavities filled with recently decayed plant remains
U3	Southern block	Inhomogeneous, non-stratified dark-brown matrix-supported gravely clay. Uniform composition and sub-angular cobble and pebbles of grains indicating small and proximal source area. Equivalent to U6 in QDF-T1 (^{14}C ages: min. 668—max. 894 Cal AD) (OSL age: 407 AD ± 230)
U2	Northern block	Plio-Quaternary bedrock 2, weathered and kaolinitized light-grey, acidic, fine-grained tuff and ash layers
U1	Southern block	Altered and weathered Plio-Quaternary bedrock 1: Volcanoclastic breccia and conglomerate, coarse grains embedded in tile red stratified tuffaceous matrix

Table 6: Radiocarbon (raw and calibrated) ages of organic rich detrital materials derived from the paleoseismic trenches samples (ETH HGB: Honggerberg, 14C Lab, ETH University Zurich, Performed by MICADAS instrument)

Sample label	ETH HGB lab. no.	Delta $^{13}C\%$	Age ± 1σ (^{14}C years BP)	(OXCAL) Calibrated age ± 2σ (95.4% confidence)	Material sampled (trench no. and sedimentary unit)
QDF-T1-C1	61041.1.1	−27.6602	1233 ± 50	781 Cal AD ± 113 yr	T1–U6
QDF-T1-C2	61042.1.1	−27.082	1825 ± 20	185 Cal AD ± 55 yr	T1–U4
QDF-T1-OC1	75058.1.1	−22.6271	444 ± 76	1517Cal AD ± 126 yr	T1–U7
QDF -T1- OC2	75059.1.1	−27.0828	1864 ± 80	150 Cal AD ± 191 yr	T1–U3
QDF-T3-OC3	75061.1.1	−21.8593	635 ± 76	1346 Cal AD ± 88 yr	T3–U3
QDF-T3-OC4	75062.1.1	−19.8332	301 ± 74	1563 Cal AD ± 121 yr	T3–U4
QDF-T3-OC5	75063.1.1	−25.0484	155 ± 75	1799 Cal AD ± 157 yr	T3–U5
QDF-T3-OC6	75064.1.1	−26.2687	274 ± 75	1571 Cal AD ± 124 yr	T3–U4

The Radiocarbon Calibrated dates are given for a 2σ (95.4%) confidence interval. For the standard deviation of the Radiocarbon raw ages, the error is ±1σ. Calibrated dates (BC/AD) were calculated using the OxCal software (Bronk Ramsey, 2017) along with the Intcal09 calibration curve (Reimer et al., 2009).

Table 7: Age of samples from alluvial terrace sediments at Sarandchay River, determined by optically stimulated luminescence method

Lab/Sample No.	CAM D_e (Gy)	MAM-3 D_e (Gy)	$^{**}\dot{D}$, Gy, ka^{-1}	CAM Age, ka	MAM Age, ka	Sedimentary unit
UNIL/QDF-t1-OSL1	10.86 ± 1.46	6.71 ± 0.94	4.16 ± 0.16	2.61 ± 0.37	1.61 ± 0.23	Alluvial terrace
UNIL/QDF-t1-OSL-2	427.70 ± 34.66	342.53 ± 52.41	3.799 ± 0.145	112.58 ± 10.09	90.16 ± 14.22	Alluvial terrace

CAM means Central Age Model; MAM-3, Minimum Age Model, 10% over-dispersion for a well-bleached population; De, Laboratory obtained equivalent dose; $^{**}\dot{D}$, Annual dose rate (amount of absorbed radiation energy per unit mass), sample with 10 ± 5% water content; Age, $D_e/\dot{D}$, the relevant information for OSL ages are presented in years BP with ±1σ errors (UNIL stands for OSL Laboratory of University Lausanne, Lausanne, Switzerland).

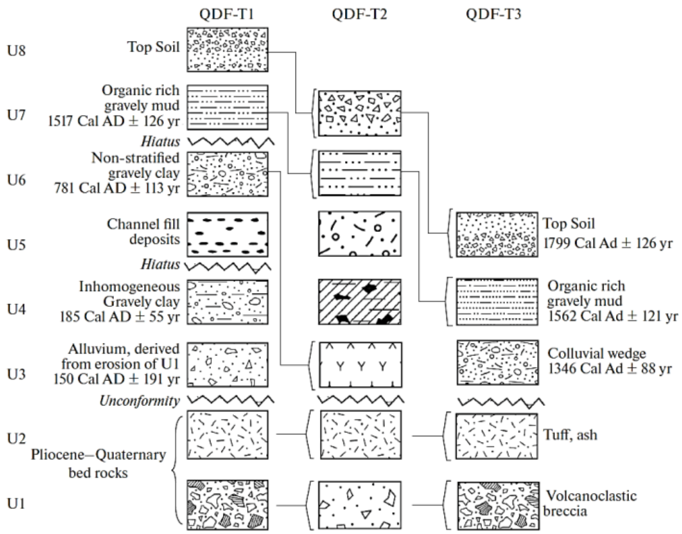

Figure 12: Correlation of bed rocks and overlying sedimentary units exposed in three studied trenches.

Table 8: Average age and seismic parameters obtained for earthquake events identified in three paleoseismic trenches

Earthquake event	Age (Cal AD)	Maximum net slip, m	Average net slip, m	Average slip per event, m	Mean recurrence interval	Slip rate, mm yr^{-1}
Most recent	2012 AD	0.99	0.79	0.84	452 yr	1.9 ± 0.1
Penultimate	1567 AD	1.46	0.90			
Ante-penultimate	1247 AD?	1.98	1.14			
Ante-ante-penultimate	≈800 AD?	0.80	0.80			
QDF-T1-E4-	≈250 AD?	0.47	0.59			
QDF-T1-E5	≈250 BC (Before 41 BC)	?	?			

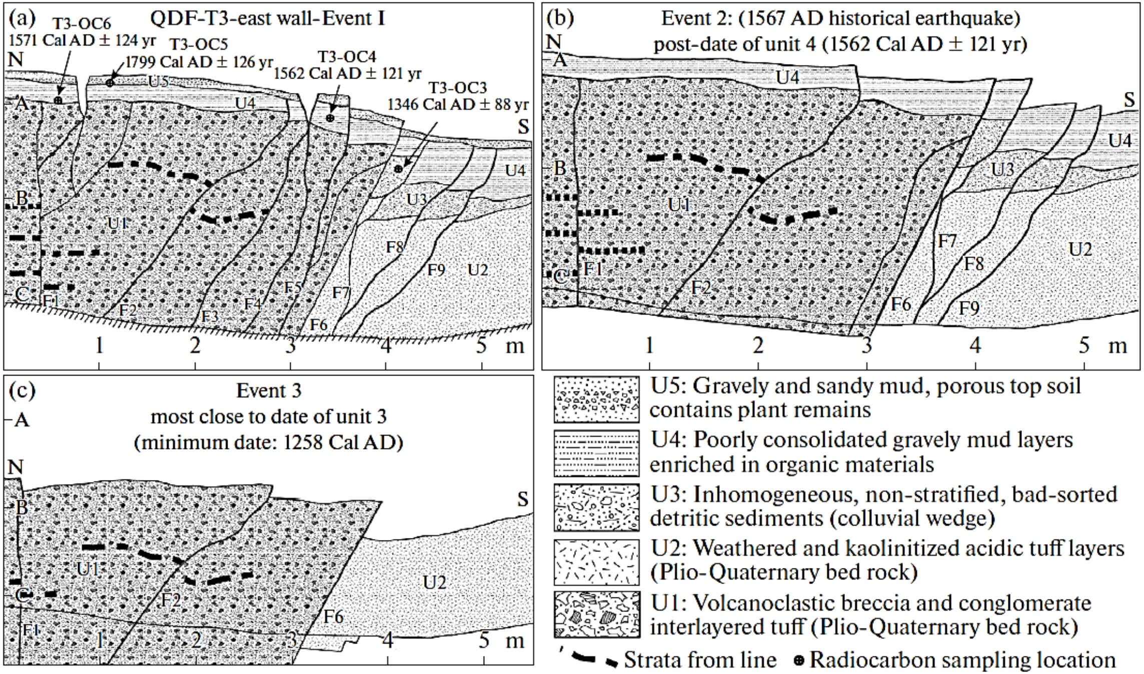
(a) QDF-T3-east wall-Event I
T3-OC6
1571 Cal AD ± 124 yr
T3-OC5
1799 Cal AD ± 126 yr
T3-OC4
1562 Cal AD ± 121 yr
T3-OC3
1346 Cal AD ± 88 yr
N
S
A
B
C
U5
U4
U3
U2
U1
F1
F2
F3
F4
F5
F6
F7
F8
F9
1
2
3
4
5 m
(b) Event 2: (1567 AD historical earthquake)
post-date of unit 4 (1562 Cal AD ± 121 yr)
(c) Event 3
most close to date of unit 3
(minimum date: 1258 Cal AD)
U5: Gravely and sandy mud, porous top soil contains plant remains
U4: Poorly consolidated gravely mud layers enriched in organic materials
U3: Inhomogeneous, non-stratified, bad-sorted detritic sediments (colluvial wedge)
U2: Weathered and kaolinitized acidic tuff layers (Plio-Quaternary bed rock)
U1: Volcanoclastic breccia and conglomerate interlayered tuff (Plio-Quaternary bed rock)
Strata from line
Radiocarbon sampling location

Figure 13: (a) Profile of QDF-T3 showing sedimentary units (U1 to U5) displaced by fault planes (F1 to F9). Sampling sites and radiocarbon age of the units are given in AD calendar. A, B and C on vertical axis have 1 m intervals. (b, c) Retro-deformational sequence in QDF-T3. Exposed units restored into their successive stages to measure horizontal and vertical displacements.

DISCUSSION AND CONCLUSIONS

The Qoshadagh Fault consists of three segments with specific structural elements, which in turn control displacement partitioning and affect the seismic behavior of the fault. The central segment has a slip rate of ≤ 2mm yr^{-1}, which is rather slow compared to the 8 mm yr^{-1} of the neighboring North Tabriz Fault.

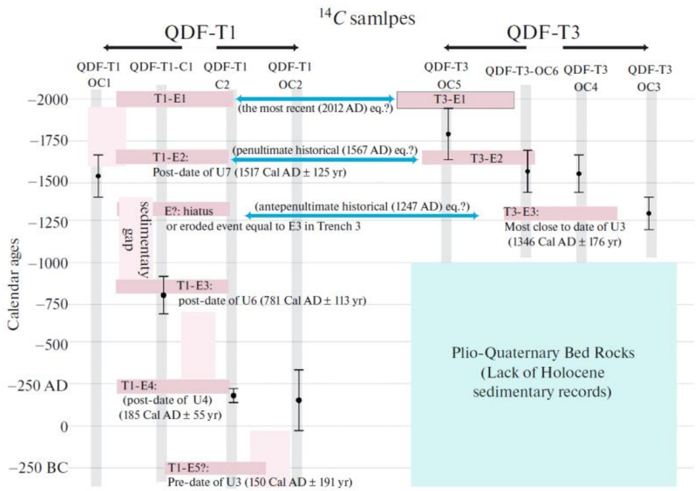

Figure 14: Age correlation of sediments and events between QDF-T1 and QDF-T3 trenches.

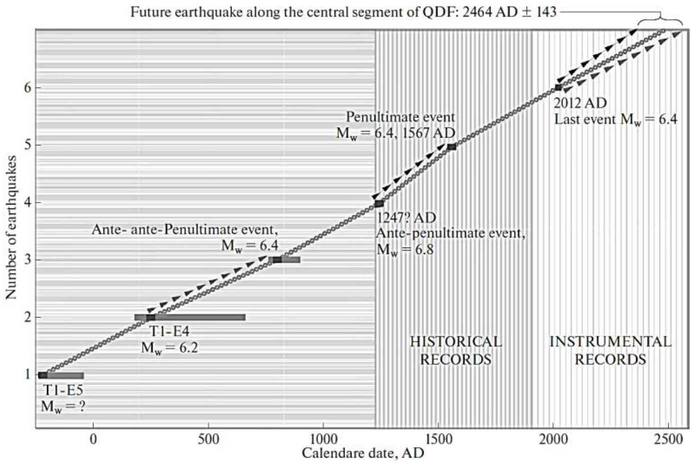

Figure 15: 2000-year-long history of QDF indicate among the correlated surface rupturing paleoearthquakes events, the minimum time interval (steeply inclined segment between the penultimate and ante-penultimate) has been 320 years and maximum value for time interval (relatively gentle gradient between ante-ante-penultimate and T1.E4) has been 550 years. Using obtained average recurrence interval of 452 ± 143 yr for the past 2 ka, the future earthquake would expect to take place approximately in 2464 ± 143 years AD.

Yet the QDF actively contributes to the regional transpressive deformation in NW Iran. The presented paleoseismic work reveals that the QDF has been responsible for several destructive earthquakes which, due to inaccurate historical records, were attributed to the North Tabriz Fault. The close proximity of the three

QDF-T1-T3 trenches permits a reliable correlation of sedimentary units and paleoseismic events (*Figure 14*,

Table 8). The eastern segment of the Qoshadagh Fault has undergone local transtension and played an important role in the volcanic activity of Mt Sabalan. The western QDF segment is connected to the Nakhichevan Fault but more field studies are required to confirm and evaluate linkage. Our investigations revealed erosion and local hiatus within the sequence of Quaternary sediments, which suggests that some rupturing earthquake events are not exposed everywhere. The OSL 2.61 ± 0.37 ka age of a strath terrace of the Sarandchay River indicates a wide sedimentary hiatus between bedrocks and overlying unconsolidated sediments. The youngest age (1799 ± 157 Cal AD) is due to ^{14}C dating of an organic-rich top soil. These two ages bracket the paleo-earthquakes identified on the central segment of the QDF. Using averaged attitude of slip vectors derived from offsets produced during the 2012 event and measured for paleo-earthquakes, we may assume similar sizes and displacements in repetitive seismic cycles of characteristic earthquakes. Calculations suggest average displacement per event (net slip) of ≈0.84 m and mean recurrence interval of 452 ± 143 years for earthquakes with a moment magnitude of $6.1 < Mw \leq 6.8$ (*Figure 15*). We also obtained an average rate of 1.7 ± 0.3 mm yr^{-1} for the past 3 ka. Although this rate seems small compared to the ≈8 mm yr^{-1} of the North Tabriz Fault, the QDF has a strong potential and represents a high seismic risk in the densely populated northwest Iran.

REFERENCES

A. Copley, M. Faridi, M. Ghorashi, J. Hollingsworth, J. Jackson, H. Nazari, B. Oveisi, and M. Talebian, “The 2012 August 11 Ahar earthquakes: Consequences for tectonics and earthquake hazard in the Turkish–Iranian Plateau”, Geophys. J. Int. 196, 15–21 (2013). Doi 10.1093/gji/ggt379

A. Ghods, E. Shabanian, E. Bergman, M. Faridi, S. Donner, G. Mortezanejad, and A. Aziz-Zanjani, “The Varzaghan–Ahar, Iran, Earthquake Doublet (Mw 6.4, 6.2): Implications for the geodynamics of northwest Iran”, Geophys. J. Int. 203, 522–540 (2015). Doi 10.1093/gji/ggv306

A. M. C. Şengor, D. Altıner, A. Cin, T. Ustaomer, and K. J. Hsu, “Origin and assembly of the Tethyside orogenic collage at the expense of Gondwana Land”, in Gondwana and Tethys, Vol. 37 of Geol. Soc. London, Spec. Publ., Ed. by M. G. Audley-Charles and A. Hallam (London, 1988), pp. 119–181.

C. Bronk Ramsey, “Methods for summarizing radiocarbon datasets”, Radiocarbon 59, 1809–1833 (2017). Doi 10.1017/RDC.2017.108

D. L. Wells and K. J. Coppersmith, “New empirical relationships among magnitude, rupture length, rupture width, rupture area, and surface displacement”, Bull. Seismol. Soc. Am. 84, 974–1002 (1994).

F. Mesbahi, M. Mohajjel, and M. Faridi, “Neogene oblique convergence and strain partitioning along the North Tabriz Fault, NW Iran”, J. Asian Earth Sci. 129, 191–205 (2016). Doi 10.1016/j.jseaes.2016.08.010.

Faridi, M., Nazari, H., Burg, J.P., Haghipour, N., Talebian, M., Ghorashi, M., Shokri, M.A., Ahmadzadeh, E. and Sahebari, S.S., 2019. Structural characteristics, paleoseismology and slip rate of the Qoshadagh fault, northwest of Iran. Geotectonics, 53, pp.280-297.

J. F. Dewey, W. C. Pitman, W. B. F. Ryan, and J. Bonnin, “Plate tectonics and the evolution of the Alpine system”, Geol. Soc. Am. Bull. 84, 3137–3180 (1973).

J. Ghalamghash, S. Z. Mousavi, J. Hassanzadeh, and A. K. Schmitt, “Geology, zircon geochronology, and petrogenesis of Sabalan volcano (northwestern Iran)”, J. Volcanol. Geotherm. Res. 327, 192–207 (2016). Doi 10.1016/j.jvolgeores.2016.05.001

K. Aki and P. G. Richards, Quantitative Seismology: Theory and Methods (Freeman, San Francisco, 1980), 2 Vols.

L.-E. Ricou, “Tethys reconstructed: Plates, continental fragments and their boundaries since 260 Ma from Central America to South-eastern Asia”, Geodin. Acta 7, 169–218 (1994). Doi 10.1080/09853111.1994.11105266

M. Alavi, “Structures of the Zagros Fold-Thrust Belt in Iran”, Am. J. Sci. 307, 1064–1095 (2007). Doi 10.2475/09.200702

M. B. Allen, J. Jackson, and R. Walker, “Late Cenozoic reorganization of the Arabia-Eurasia collision and the comparison of short-term and long-term deformation rates”, Tectonics 23 (2004). Doi 10.1029/2003TC001530

M. B. Allen, M. Kheirkhah, I. Neill, M. H. Emami, and C. L. Mcleod, “Generation of arc and within-plate chemical signatures in collision zone magmatism: Quaternary lavas from Kurdistan province, Iran”, J. Petrol. 54, 887–911 (2013). Doi 10.1093/petrology/egs090

M. Faridi and A. Sartibi, Preliminary Report on 11 August 2012 Varzegan-Ahar Earthquake: Internal Report with Surface Rupture Map and Intensity Map Attachments (Geol. Surv. Iran, NW Reg. Off., 2012).

M. Faridi and E. Haghfarshi, Geological Map of Khoja, Sheet No. 5366, Scale 1 : 100000 (Geol. Surv. Iran, 2006).

M. Faridi, J. P. Burg, H. Nazari, M. Talebian, and M. Ghorashi, “Active fault pattern and interplay in Azerbaijan Region (NW Iran)”, Geotectonics 51, 428– 437 (2017).

M. Faridi, Structural Geology of Mount Sabalan: Internal Report (Iran. Org. Renewable Energy, 2010).

M. Rizza, P. Vernant, J. F. Ritz, M. Peyret, H. Nankali, H. Nazari, Y. Djamour, R. Salamati, F. Tavakoli, J. Chery, S. A. Mahan, and F. Masson, “Morphotectonic and geodetic evidence for a constant slip-rate over the last 45 kyr along the Tabriz fault (Iran)”, Geophys. J. Int. 193, 1083–1094 (2013). Doi 10.1093/gji/ggt041

M. Zare, A Review on Ardabil 28 February 1997 Earthquake (Int. Inst. Seismol. Earthquake Eng., 1997).

P. Agard, J. Omrani, L. Jolivet, H. Whitechurch, B. Vrielynck, W. Spakman, P. Monie, B. Meyer, and R. Wortel, "Zagros orogeny: A subduction-dominated process", Geol. Mag. 148, 692–725 (2011). Doi 10.1017/S001675681100046X

P. J. Reimer, M. G. Baillie, E. Bard, A. Bayliss, J. W. Beck, P. G. Blackwell, C. Bronk Ramsey, C. E. Buck, G. S. Burr, R. L. Edwards, M. Friedrich, P.M. Grootes, T. P. Guilderson, I. Hajdas, T. J. Heaton, et al., "IntCal09 and Marine09 radiocarbon age calibration curves, 0–50,000 years cal BP", Radiocarbon 51, 1111–1150 (2009).

P. Vernant, "What can we learn from 20 years of interseismic GPS measurements across strike-slip faults", Tectonophysics 644–645, 22–35 (2015). Doi 10.1016/j.tecto.2015.01.013

S. McClusky, S. Balassanian, A. Barka, C. Demir, S. Ergintav, I. Georgiev, O. Gurkan, M. Hamburger, K. Hurst, H. Kahle, K. Kastens, G. Kekelidze, R. King, V. Kotzev, O. Lenk, et al., "Global Positioning System constraints on plate kinematics and dynamics in the eastern Mediterranean and Caucasus", J. Geophys. Res.: Solid Earth 105, 5695–5719 (2002). Doi 10.1029/1999JB900351

T. C. Hanks and H. Kanamori, "A moment magnitude scale", J. Geophys. Res., B 84, 2348–2350 (1979). Doi 10.1029/JB084iB05p02348

V. G. Trifonov and I. Kozhurin, "Study of active faults: Theoretical and applied implications", Geotectonics 44, 510–528 (2010).

V. G. Trifonov, "World map of active faults (preliminary results of studies)", Quat. Int. 25, 3–12 (1995).

Y. Zoka, The Earthquakes of Tabriz (Ketabsara, Tehran, 1989). 28. M. Zare, A Review on Ardabil 28 February 1997 Earthquake (Int. Inst. Seismol. Earthquake Eng., 1997).